Structural, optical, magnetic and electrical properties of zinc oxide doped with iron: A review

Abstract

This review studied the structural, optical, magnetic and electrical properties of zinc oxide doped with iron. ZnO is an excellent nanomaterial in semiconductor industries because of its properties such as low cost, high stability and high absorbance. However, some major limitations such as toxicity, low photocatalytic ability in UV rays and quick recombination of hole – electron pairs has affected its application. Hence, doping has proven essential in overcoming these limitations. The structure of zinc oxide is determined by X-ray diffraction (XRD). The Xray diffraction studies show that the structure is hexagonal with wurtzite structure, ZnO films prefer to grow in the (002) direction this is because each apex is parallel to the c-axis in the wurtzite structure. The optical properties investigated which include the absorbance and transmittance spectra, energy band gab, absorption coefficient, and other optical constants. The results showed that films have direct optical transition. The optical band gab was found to be in the range to (3.26 – 3.35) eV. The electrical properties of these films have been studied, it was reported to have low resistivity and consequently high electrical conductivity at high dopant iron concentration consequently, higher electrical resistivity was observed with lower conductivity at lower dopant concentration. At higher iron-doped ZnO (x = 0.10 and 0.20) samples exhibited obvious ferromagnetic behaviors this implies that the saturation magnetization of Zn1-xFexO nanoparticles increases with the increasing of Fe doping concentration compared with pure ZnO. Hence the SEM of iron-doped zinc oxide nanaoparticles consists of ellipsoidal shape particles, which are well dispersed with smooth surface and uniform size.

Keywords: Optical Properties, Structural Properties, Magnetic Properties, ZnO.

1.0 Introduction

Nanoparticles are micro particles whose particles are usually less than 100nm (Onu et al. 2023). Hence, the development of improved nano-composite materials is gaining global attention among scientists because of the numerous applications of the materials. Currently, there is ongoing extensive research on the synthesis of essential and vital third generation semiconductor nano-particles that will have comprehensive relevance on account of their multi-functional characteristics (Faramawy et al. 2022). These nano-composites have copious importance in semiconducting industries, optoelectronic industries and photocatalytic industries (Madkhali et al. 2022). Furthermore, they can be applied in the environmental field for water treatment, gas sensors, solar photocatalysis, etc (Theerthagiri et al. 2019; Hamid et al. 2017; Kumar et al.

2015); in electro-optical fields for solar cells, optical waveguides, light-emitting devices etc (Hwang et al. 2007); in biological fields for biomedical and antibacterial purposes, biosensors etc (Tereshchenko et al. 2016); in electronics for light emitting diode, thin film transistors, etc (Kumar et al. 2015).

2.0 Zinc oxide nano-particles

Zinc oxide (ZnO) is an n-type semi-conductor nano-particle that have many important that have wide spread applications across different industries (Dhiman et al. 2013; Faramawy et al.2022). This is mainly because of its exceptional chemical and physical characteristics, such as a large direct energy gap (e.g., 3.37 eV at 300 K), excellent conditions of ultraviolet and blue emissions, and a large excitation binding energy (60 meV) at room temperature, which makes it superior to numerous other nanomaterials (Rong et al. 2018). Besides, ZnO is environmental friendly and has hexagonal wurtzite (WZ) which is relatively stable. It has ability to alter electrical conductivity of gaseous samples. Also, ZnO has outstanding properties such as low cost, high stability, with intrinsic ability to absorb UV radiations (Madkhali et al. 2022; Liu et al. 2011). The remarkable morphological features of ZnO make it a striking material that is widely used as a counterpart of a noteworthy scope of applications. However, there are significant drawbacks in the application of ZnO nanoparticles. These drawbacks mitigate the effective application of ZnO nano-particles for industrial purposes. The most important one is their toxicity. The toxic effects are usually due to their high solubility which leads to cytotoxicity and oxidative stress (Carofiglio et al. 2021). Besides, the optical, electrical and structural properties of pure ZnO nano-particles limits its application. Moreover, the wide band gap of the ZnO nanoparticles depicts low photocatalytic ability in UV rays. Quick recombination of the hole-electron pairs is another major constraint of the ZnO nanoparticles (Ebrahimi et al. 2019; Xu et al. 2010). These drawbacks can be overcome with required improvement in the properties of the ZnO through doping of the ZnO nanoparticles with transition metals.

3.0 Properties of iron doped zinc oxide

Doping is the process of adding an ion that wasn't initially present in the starting material into a crystal lattice. Doping of ZnO with transition metals have the capability of decreasing the heat conductivity while simultaneously increasing the electrical conductivity of the nanoparticle

(Pashkevich et al. 2018). Doping can also be very helpful in modifying the energy band-gap, which will directly affect the photocatalytic capabilities of ZnO. Doping is a potent technique for changing the electrical and optical characteristics of semiconducting materials like ZnO (Carofiglio, et al. 2021). Doping ions cause the creation of novel electronic transitions between energy levels and more defect states in the energy band structure which mar result to a decrease in the bandgap of the ZnO and an extension of the matching absorption spectral area from the UV to visible light. The purest form of ZnO exhibits diamagnetic properties but the magnetic properties can be enhanced with doping (Carofiglio et al. 2020). Doping with transition metals such as iron can stimulate the alteration from diamagnetism to paramagnetism and ferromagnetism (Ravichandran et al. 2014; Santo et al. 2012; Xu et al. 2009). With the enhanced magnetic properties, the doped ZnO can be applied in bio-imaging processes such as magnetic resonance imaging (MRI) (Carofiglio, et al. 2021). The characteristics of these materials depend not only on the impurity concentration that has been incorporated, but also on whether the impurities are uniformly distributed in the matrix lattice (wurtzite) or form submicron-sized magnetic clusters that have a particular phase and magnetic structure.
The properties of iron-doped ZnO are categorized into structural properties, optical properties, magnetic properties and electrical properties.

4.0 Structural properties

The structural properties of the iron-doped ZnO are usually investigated using X-ray diffraction (XRD), scanning electron microscopy (SEM) and Scanning electron microscopy-energy dispersive X-ray (SEM-EDX). Furthermore some properties such as crystalline size, dislocation density, unit cell volume are used to study the structural properties of the iron-doped ZnO. Other properties such as include x-ray density, lattice parameters and lattice strain can also reveal additional properties of the nano material.

4.1 Scanning Electron Microscopy (SEM)

Scanning Electron Microscopy (SEM) is a surface imaging method in which the incident electron beam scans across the sample surface and interacts with the sample to generate backscattered and secondary electrons that are used to create an image of the sample. It is a test process that scans a sample with an electron beam to produce a magnified image for analysis. The method is also known as SEM analysis and SEM microscopy, and is used very effectively in

microanalysis and failure analysis of solid inorganic materials. Scanning electron microscopy-energy dispersive X-ray analysis (SEM-EDX) provides a quick nondestructive determination of the elemental composition of the sample readily identifying barium, potassium, strontium, and chlorine.

Wu et al. (2014) observed the morphology and microstructure of the iron doped ZnO nanoparticles through High-resolution transmission electron microscopy (HRTEM). This provides direct images of the atomic structure of the samples, hence it is possible to have direct information about the crystallographic structure of materials from images. High phase contrast images as small as a crystal cell can be acquired via this method.

The images of the iron-doped zinc oxide nano-particles (Zn0.95Fe0.05O) reveal the presence of randomly distributed ellipsoidal shaped nanoparticles (Figure 1). The iron-doped zinc oxide nanaoparticles consists of ellipsoidal shape particles, and well dispersed with smooth surface and uniform size. The diameter of the nanoparticles ranged from 10 to 40 nm, with an average diameter approximately 25 nm. The crystalline quality improved with the iron doping. The resolved lattice plane extending through the image confirms that the particle is crystallized with clear lattice fringes. The interplanar distance is about 0.263 nm which is in good agreement with the d-spacing of (002) planes of hexagonal wurtzite ZnO structure. The value of lattice spacing is greater than that of pure ZnO (0.26 nm). The HRTEM analysis is consistent with the XRD results, which further indicates that all the Fe ions successfully substituted for the lattice site of Zn2+ in the hexagonal wurtzite structure and no impurity phase appeared (Wu et al. 2014).

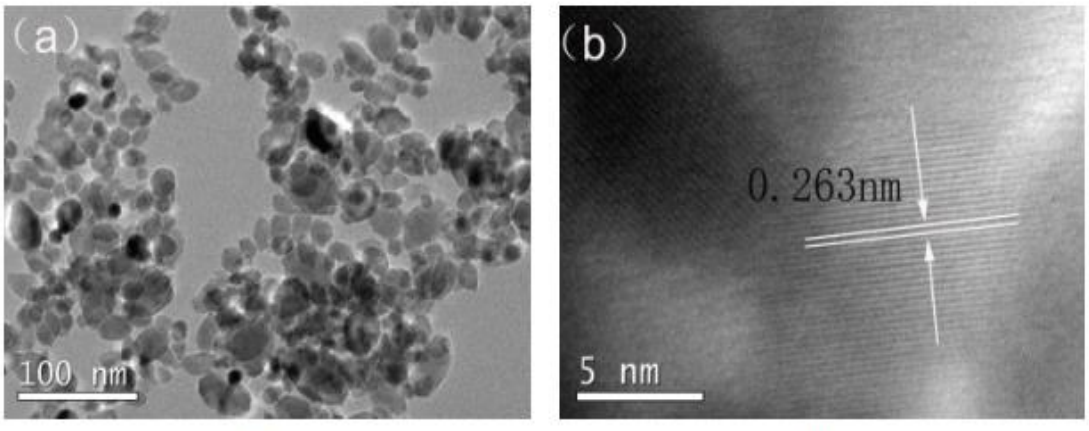

Figure 1: HRTEM images of $Zn_{0.95}Fe_{0.05}O$ nano-particles (Wu et al. 2014)

In the morphology analysis of the ZO and Fe doped ZO thin films, Faramawy et al. (2022) observed that the pure zinc oxide film surface seems to be agglomerated and spherical in shape. The surface of the films consists of tightly packed grains forming a smooth surface without any voids and cracks whereas the Fe doped zinc oxide films look like black and white islands of spherical shape. Still, by increasing the DC deposited power for Fe with ZO deposition, the black spots decreased. A SEM image of the sectional view of the samples could help in discovering the shape of the spherical grains and their interface with the substrate. Moreover, the shape of the grains would be hard to identify because the growth could not be described in a reliable way. Further, the distribution and size in grains is inhomogeneous. The observed peaks are attributed to zinc, oxygen and iron as principal elemental components with no other impurities being obtained. The Zn:O:Fe atomic percentage ratios of the ZO thin film are listed.

The elemental composition of the iron-doped zinc oxide nanoparticles (synthesized though hydrothermal method) can be determined via energy dispersive X-ray analysis (EDS). Wu et al. (2014) reported that the synthesized iron-doped zinc oxide nanoparticles confirmed the presence of mainly iron, zinc, and oxygen with traces of copper and carbon (which probably oringated from from the TEM micromesh grid). They reported that the characteristic peaks of O appeared at 0.5 keV, the characteristic peaks of Zn appeared at 1 and 8.7 keV while that of Fe was at 0.7, 6.4, and 7.1 keV. Also the characteristic peaks of Cu appeared at 0.9, 8 and 8.9 keV. The result confirmed that Fe-doped ZnO diluted magnetic semiconductor was successfully synthesized by hydrothermal method and Fe3+ in the sample occupied the place of Zn2+ (Wu et al.2014).
In the EDX spectrum ZO and Fe doped ZO thin films, Faramawy et al. (2022) reported that the observed peaks are only attributed to zinc, oxygen and iron as principal elemental components with no other impurities being obtained.

4.2 Photoluminescence analysis

Photoluminescence (PL) can be used to determine the structure of the nanoparticles. Both the iron-doped zinc oxide nanoparticles and the pure zinc oxides were compared by Wu et al. (2014) as shown in Figure 2. The pure ZnO sample contains six main emission peaks, including three obvious broad bands centered at 390, 440, and 490 nm and three comparatively weak emission

peaks at 420, 460, and 525 nm, respectively. The 1% sample exhibits similar emission to pure ZnO. This illustrates that the Zn 0.99Fe0.01O sample displays nearly the same structure of pure ZnO. But the emission peak position of doped sample exhibits a slight blue shift with the increase of Fe3+ concentration, and this is attributed to defects or the oxygen vacancies in ZnO induced by Fe3+ doping. In addition, the visible light (VL) emission band is also suppressed with the increase of the Fe3+ concentration.

The strong ultraviolet (UV) emission band at 390 nm (3.18 eV) and the weak violet emission peak located at 420 nm (2.95 eV) originate from excitonic recombination corresponding to the near-band-edge emission (NBE) of wide band gap of ZnO, because of the quantum confinement effect. The strong blue emission bands centered at 440 nm (2.8 eV) and the weak blue emission peak at 460 nm (2.69 eV) are attributed to the transitions between the shallow donor levels of the interstitial Zn to the top of the valence band or the transitions between shallow acceptor levels of oxygen vacancies and shallow donor levels of zinc vacancy. The blue-green bands centered at 490 nm (2.55 eV) for samples are ascribed to the transition between the deep donor level of oxygen vacancy, which is close to the bottom of the conduction band of about 0.8~0.9 eV, to the valence band. The weak green emission peak at 525 nm (2.36 eV) is possibly assigned to positively charged electron transition and surface traps mediated by defects in the band gap. PL spectrum analysis further illustrates that Fe ions are probably incorporated into the ZnO host matrix in the doped ZnO sample.

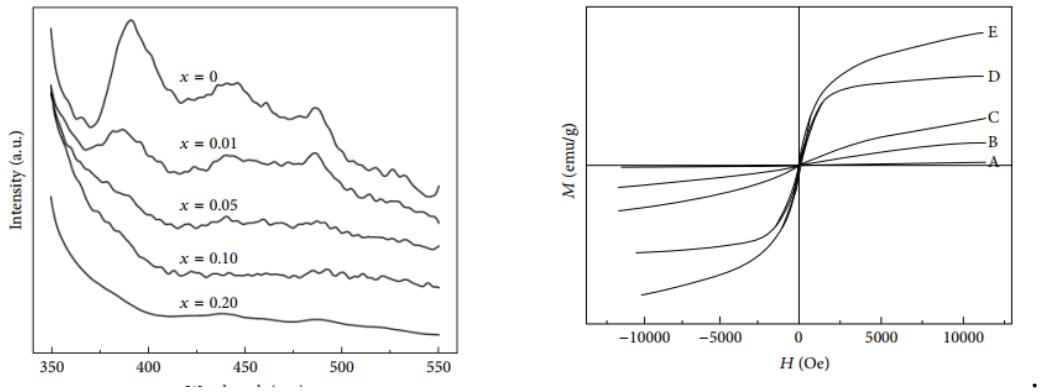

Figure 2: Photoluminescence spectra of the Zn1-xFexO nanoparticles.

4.3 X-ray diffraction (XRD)

XRD is a scattering of X-rays by the atoms of a crystal that produces an interference effect so that the diffraction pattern gives information on the structure of the crystal or the identity of a crystalline substance. Ashraf et al. (2015) reported that there is no change in the wurtzite structure of ZnO after iron doping hence complete doping of iron was obtained. The full width at half maximum increased with increase in iron doping concentration as shown in Figure 3..

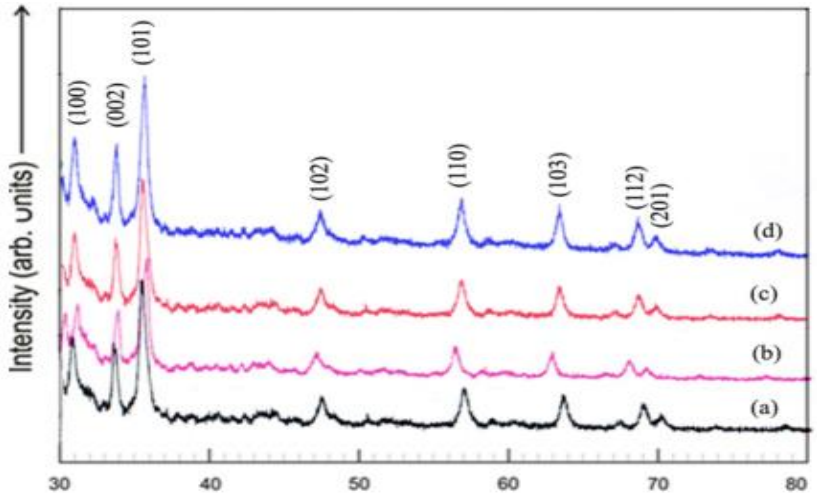

Figure 3. XRD of the un-doped (a) and iron doped ZnO nanoparticles with variation of iron content (b) 2, (c) 6 and (d) 10 wt% (Ashraf et al. 2015)

It is possible that all the diffraction peaks can be well corresponding to the diffractions of (100), (002), (101), (102), (110), (103), (200), (112), (201), and (202) planes of single-phase hexagonal wurtzite structure with the space group 6_3mc, respectively (Wu et al. 2014). The diffraction peaks are in excellent harmony with the values of the standard spectrum. Besides, there are no traces of impurity or secondary phases within the detection range of XRD and there are no obvious diffraction patterns of Fe species such as Fe, Fe_2O_3, and Fe_3O_4 in the samples where the doping atomic percentage is from 1% to 20%. These results indicate that all Fe ions were incorporated in the lattice of the host crystals, the products consist of pure phase, and no characteristic peaks can be found from other impurities (Wu et al. 2014).

For Fe-doped ZnO dilute magnetic semiconductors, the peak position of the doped ZnO samples shifts to lower angles compared with pure ZnO, and also there is a decrease in the intensity of peaks with the Fe doping concentration. This shifting as well as decrease in intensity of the

characteristic peak clearly indicates the successful incorporation of Fe in the ZnO matrix, which can be attributed to the difference of ion radius of Zn2+ (0.74 A) comparing with that of Fe ˚ 3+ (0.64 A). ˚ It is indicated that Fe ions occupy the Zn ions sites in the hexagonal wurtzite structure and no impurity phase appears (Wu et al. 2014).

According to Faramawy et al. (2022), zinc oxide nanoparticles exhibited preferential (002) c-axis orientation, which grew perpendicular to the substrate surface. This meant that the sputtered ZO and ZnOFe thin films with a c-axis have a preferential orientation due to the lowest surface free energy of (002) plane in ZO. In the equilibrium state, the films grow with the plane of the lowest surface free energy parallel to the surface if there is no effect from the substrate. Additionally, the sp3 hybridized orbit in zinc oxide forms a tetrahedral coordination. Because each apex is parallel to the c-axis in the wurtzite structure, ZO films prefer to grow in the (002) direction (Fujimura et al. 1993).

4.4 Crystalline size

The crystallite size "D" for iron doped ZnO nanoparticles was calculated using the Debye–Scherer formula given in equation (1)

$$D = \frac{0.9\,\lambda}{\beta \cos\theta} \qquad (1)$$

Where, β is full width at half-maximum, λis the X-ray wavelength and θ is Bragg's diffraction angle.

It can be seen from Figure 4 that there is a decrease in the crystallite size (29-19nm) of the zinc oxide nano particles with increase in the quantity of iron doping observed (Ashraf et al. 2015).

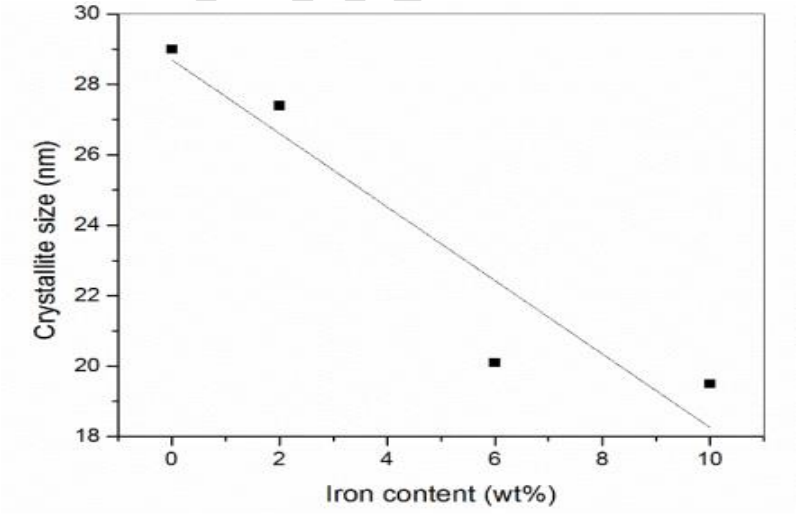

Figure 4. Variation of Crystallite size of the iron doped ZnO nanoparticles (Ashraf et al. 2015)

4.5 Dislocation density

Dislocation density has been found to increase with increase in the iron content of the doped ZnO nanoparticles. Dislocation density was calculated by using formula $\frac{1}{D^2}$. There was linear increase in dislocation density with increase in the iron content of the doped ZnO (Figure 5).

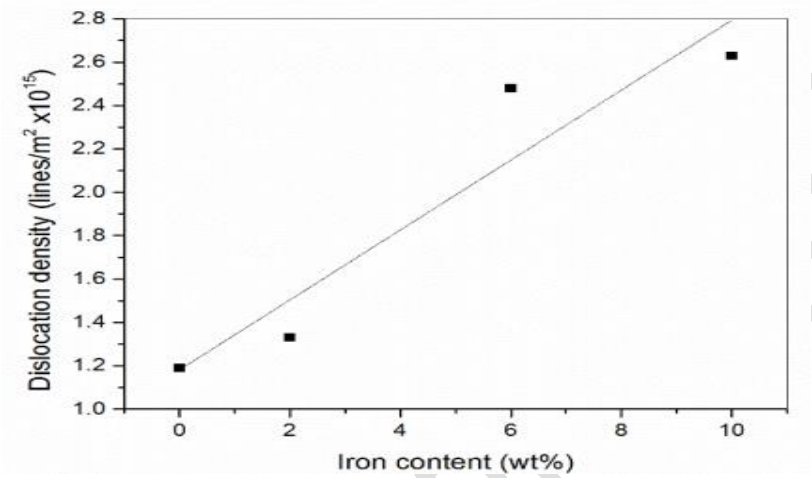

Figure 5. Effect of iron doping on the Dislocation density of the doped ZnO nanoparticles (Ashraf et al. 2015)

4.6 Unit volume

It was observed that there is usually a decrease in lattice parameter and therefore unit cell volume as the concentration of the iron concentration increase in the doped zinc oxide nano particle. This is mainly because of the difference in ionic radii of zinc and iron ions (Ashraf et al. 2015).

5.0 Magnetic properties

5.1 Magnetization

Room temperature ferromagnetism was usually observed for iron doped zinc oxide. There was increase in saturation magnetization with increase in dopant concentration of iron as shown in Figures 6 and 7 (Ashraf et al. 2015). However, even undoped nanoparticles can show ferromagnetic behavior. The existence of Zn vacancies causes the oxygen 2p orbitals to spin

polarize, which causes this effect. Ruderman–Kittel–Kasuya–Yoshida interactions (RKKY) interactions led to a rise in saturation magnetization as iron was doped in the host lattice. These interactions come up as a result of free carriers oscillating across large distances. Saturation magnetization was increased from 0.065 to 0.088 emu/g with increase in doping concentration (Ashraf et al. 2015). In addition to the Fe doping ions, the presence of lattice defects such as strain and texture may also contribute significantly to the room temperature magnetic properties (Faramawy et al. 2022; Pan et al. 2007). Ferromagnetism in transition metal doped zinc oxide may be because of secondary magnetic phases or due to the oxidation of Fe in mixed valence (Fe2+ and Fe3+) states (Wang et al. 2010; Kumar et al. 2009).

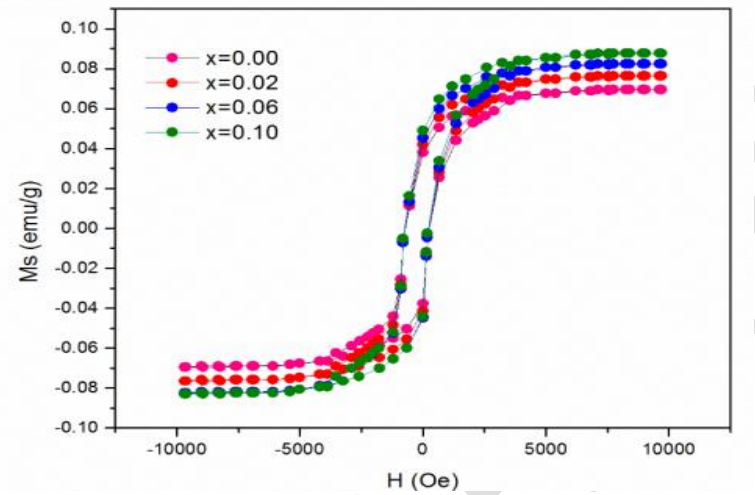

Figure 6. M–H curves of iron doped ZnO nanoparticles with variation of iron concentration

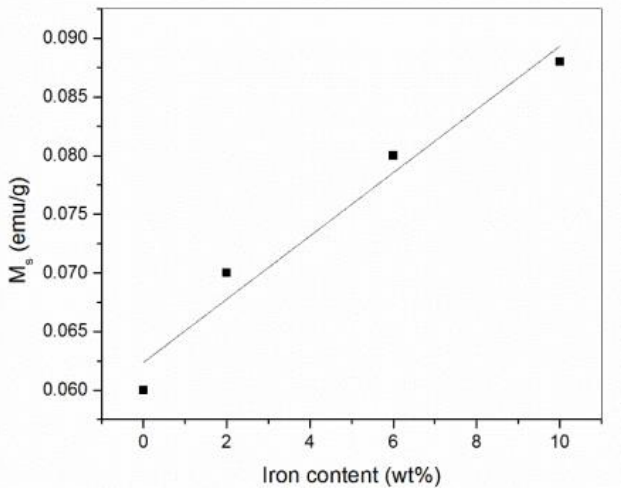

Figure. 7. Saturation magnetization of iron doped samples at various doping concentration (Ashraf et al. 2015)

5.2 Magnetic hysteresis

Wu et al. (2014) also reported on the magnetic hysteresis (M–H) loops of the Zn1-xFexO nanoparticles with different doping consistency (x = 0, 0.01, 0.05, 0.10, and 0.20) measured at room temperature. The magnetic hysteresis loops of ZnO and lower doped ZnO (x = 0.01 and 0.05) samples pass origin of coordinates, and the remanent magnetization (Mr), and coercivity (Hc) are zero. It implied that these samples show paramagnetic behaviors at room temperature. The saturation magnetization values are 0.74 emu/g and 1.74 emu/g and the coercive force values are 90 Oe and 78 Oe, respectively, for ZnO (x = 0.10 and 0.20). It is evident that a transition from the paramagnetic state to the ferromagnetism state occured. The saturation magnetization of Zn1-xFexO nanoparticles increases with the increasing of Fe doping concentration compared with pure ZnO

The room temperature ferromagnetism of the Zn1-xFexO nanoparticles could arise from two possible sources. One is extrinsic magnetism and the other is intrinsic magnetism. Extrinsic source includes the formation of clusters of transition elements or secondary phase. Exchange interactions come under intrinsic source of magnetism. But the XRD results of the Zn1-xFexO nanoparticles suggest no traces of impurity or secondary phases (these parasitic phases include the Fe clusters and any other phases like Fe_2O_3, Fe_3O_4, etc.). Thus, the possibility of ferromagnetism due to the clusters of transition elements or secondary phases in the samples could be ruled out. Hence, the obtained ferromagnetism is an intrinsic magnetic property of the Zn1-xFexO nanoparticles.

It is evident from the XRD analysis that Fe is incorporated into the ZnO lattice. In view of the Fe3+ ions substituted into ZnO lattice, the origin of magnetism in the samples is due to the exchange interaction between local spin polarized electrons (such as the electrons of Fe3+ ions) and the conductive electrons. Such interaction can lead to the spin polarization of conductive electrons. Consequently, the spin-polarized conductive electrons undergo an exchange interaction with local spin-polarized electrons of Fe3+ ions. Thus, after a successive long-range

exchange interaction, almost all Fe3+ ions exhibit the same spin direction, resulting in the ferromagnetism of the material (Elilarassi and Chandrasekaran, 2012).

The presence of lattice defects as strain and texture, and concentration of Fe doping ions may also have a major impact on the room temperature magnetic properties.

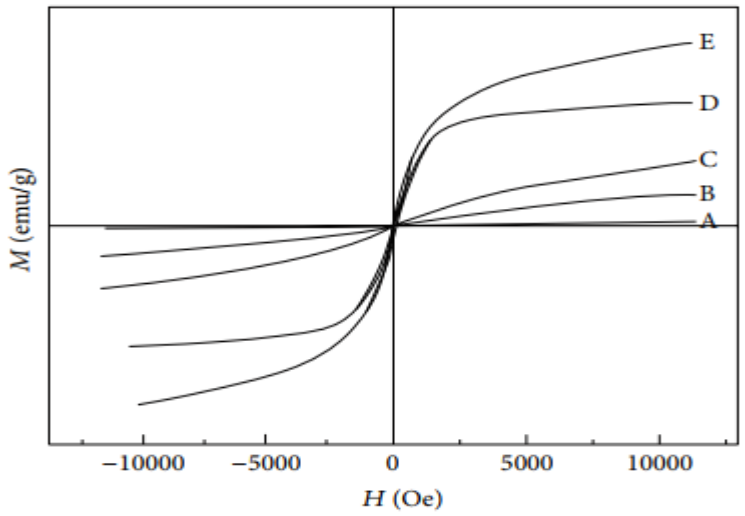

Figure 8: The magnetic hysteresis loops of the Zn1-*x*Fe*x*O nanoparticles. (Wu et al. 2014)

6.0 Optical properties

6.1 Transmittance Spectra

This is usually the ratio of the transmitted power I (λ) to the incident power I_o (λ) in a tiny wavelength interval around the center wavelength λ and in a certain (sufficiently small) solid angle of aperture.

Samples of zinc oxide and zinc oxide with iron doping are transparent to visible and infrared light when grown on silicon dioxide, therefore transmittance spectra and observations of the material's characteristics can easily be obtained. According to Faramawy et al. (2022), the pure ZnO and the iron-doped ZnO nanoparticles films' optical transmittance spectra displayed high transmission in the visible spectrum and a significant decline in the UV spectrum, which is

where the band gap is located (Figure 9). The interaction of the incident long wavelength radiation with the free electrons in the films is what causes the reduction in transmittance (Yusuf et al. 2019). Besides the films also exhibit strong transmission in the visible area of the spectrum, which ends at shorter wavelengths, but there is a clear absorption in the UV region that became more pronounced with increasing Fe concentration.

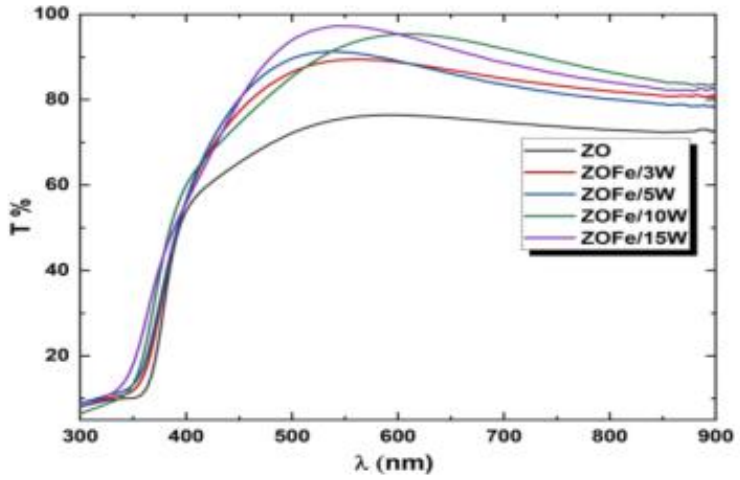

Figure 9. Transmittance of ZnO and ZnOFe thin films (Faramawy et al. 2022)

6.2 Optical band energy gap

The optical band gap energy (E_g) is defined as the sum of the bulk band gap energy, the electron and hole confinement energies. It is the minimum energy required to make an electron pairing in the semi-conductor. The optical bandgap is the threshold for photons to be absorbed. The different methods of evaluating optical band gap energy include Tauc method, Logarithmic derivative (LD) method, The derivative of transmittance (T) against photon energy (hn), The derivative of transmittance (T) against wavelength (λ) among others (Faramawy et al. 2022).

Values of E_g increased from the pure ZnO nanoparticles to the doped ZnO nanoparticles.

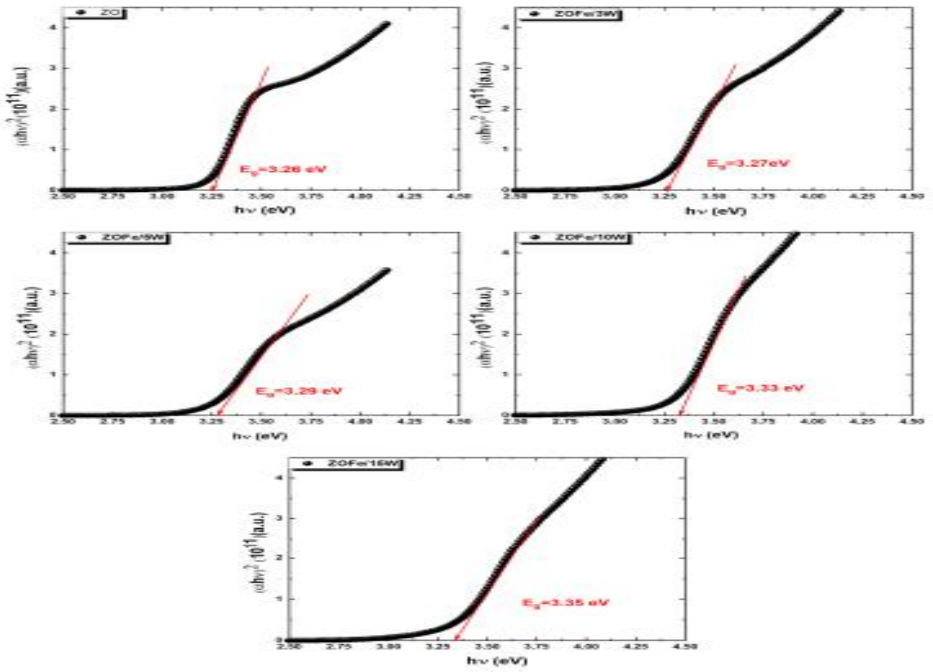

Figure 10. Plot of (*ahn*)2 vs. (*hn*) for the undoped and Fe doped ZnO thin films. Faramawy et al. (2022)

The incidence of a photon with energy of h_n on a semiconductor leads to a transition between the highest occupied state of valence band and the lowest unoccupied state of the conduction band. Furthermore, as the doping concentration of Fe increases, the E_g value increases (Figure 10). The optical band gap energy is mainly dependent on the valency of Fe ions in an iron doped ZnO nanoparticles (Salem et al. 2016). The optical characteristics of ZnO thin films are significantly influenced by the valence state of Fe. Iron dopants in ZnO thin films can occur in either of the two forms, Fe2+ or Fe3+, or even simultaneously in some cases. There is a lot of variation in the optical performance of Fe-doped ZnO thin films, which produces contradictory results sometimes (Faramawy et al. 2022). By incorporating Fe onto ZnO films, the valence band's maximum is raised and the conduction band's minimum is lowered, which reduces the band gap. Wang et al. (2009) and Chen et al.(2007) reported that increase in the Fe doping concentration in ZnO nanoparticles can reduce the band gap. However, when Fe3+ ions are substituted for Zn2+ ions, this leads to increase in the concentration of extra free carriers. Consequently, the band gap

increases and the Fermi level shifts closer to the conduction band. This makes the optical band gap of Fe-doped ZO thin films tunable.

The absorption spectrum of a pure semiconductor is known to be dramatically altered by doping, leading to degenerate energy levels that cause the Fermi level to rise over the conduction band edge. This change is referred to as a Moss-Burstein shift and is caused by doping-induced band-filling. It leads to significant increase in the band gap energy from the undoped to doped nanoparticle films (Dhiman et al. 2013; Shanmuganathan and Banu, 2014).

6.3 Urbach Energy

The Urbach energy (E_u) evaluates the degree of structural disorderliness of the nano-films (Faramawy et al. 2022). The imperfection in the structurally disordered film leads to broadening the bands of localized states. The Urbach energy increases as the Fe concentration increased (Figure 11). Fe doping is followed by an increase of the strain which can also create structural disorder. The dopant may contribute significantly to the width of localized states within the ZO's optical band. Hence, the Urbach energy is responsible for the valence and conduction bands' tails (Shaban et al. 2017).

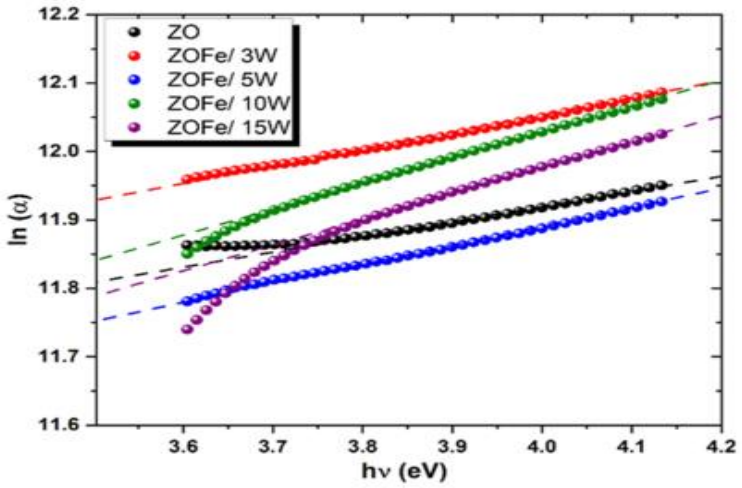

Figure 11. ln (α) vs. (*hn*) to determine the Urbach energy of ZO and Fe doped ZO thin films (Faramawy et al. 2022)

6.4 Refractive index

In optical science, refractive index of an optical medium is a dimensionless number that indicates the light-bending capability of the said medium. It determines the quantity of light that is refracted when incident on a material. The refractive index in the semiconductor is a measure of

its transparency to incident spectral radiation. Refractive index decreases from the undoped to the doped ZnO nano films. Furthermore, increasing the iron content of an iron doped ZnO nanoparticles will result to increase in the refractive index of the nanoparticles (Faramawy et al. 2022).

6.5 Extinction coefficient

The extinction coefficient, k, is a characteristic that determines how strongly a species absorbs or reflects radiation or light at a particular wavelength. It is an intrinsic property of the isolates that is dependent on its atomic, chemical, and structural composition. The extinction coefficient reflects the absorption of electromagnetic waves in the semiconductor due to inelastic scattering events (Faramawy et al. 2022).

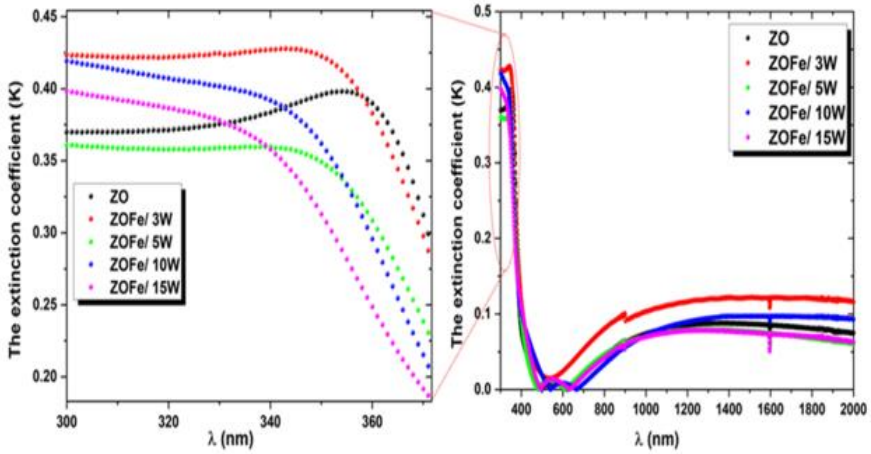

Figure 12. The extinction coefficient (K) as a function of the wavelength (λ) for the undoped and Fe doped ZnO films (Faramawy et al. 2022) .

The values of the extinction coefficient are usually very small and relatively constant in most of the visible region. This indicates the smoothness on the surface and homogeneity of the films and enhances its uses in blocking UV radiation (Shanmuganathan and Banu, 2014). Extinction coefficient increases with increase in the iron concentration of doped ZnO nanoparticles. Increase in extinction coefficient value by doping Fe can be ascribed to increasing topical donor levels formed within the energy levels that lead to an increased extinction coefficient, showing that the electronic transitions occur directly (Faramawy et al. 2022).

7.0 Electrical properties

7.1 Electrical conductivity and electrical resistivity

Electrical conductivity (EC), σ, is a measure of a material's ability to carry an electrical current. It is also defined as how much voltage is required to get an amount of electric current to flow. This is largely determined by the number of electrons in the outermost shell; these electrons determine the ease with which mobile electrons are generated. Zinc oxide nano particles have low electrical conductivity (Faramawy et al. 2022). Doping zinc oxide with transition metals is one of the major ways of improving the electron transport rates and subsequently increase the electrical conductivity (and reduce the electrical resistivity) in the nano particles (Ueda et al. 2001).

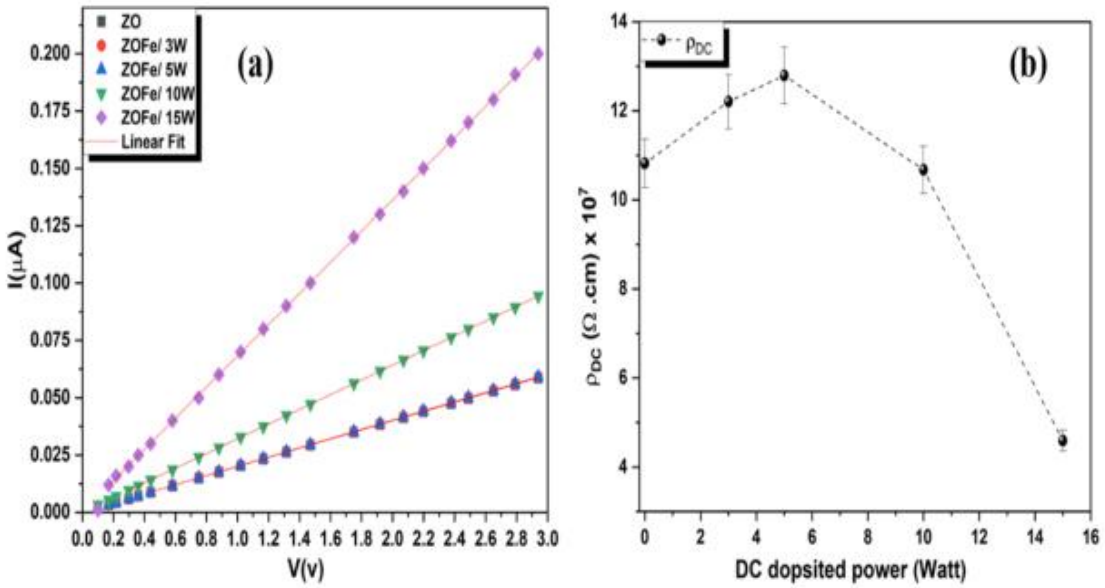

Figure 13. (a) I-V characteristics of undoped and Fe doped ZO thin films and (b) variations of the electrical resistivity ρDC with Fe concentration of all investigated thin films. Faramawy et al. (2022)

Faramawy et al. (2022) reported low resistivity (and consequently high electrical conductivity) at high dopant iron concentration. Cherif et al (2016) also reported similar trend of higher electrical resistivity (lower conductivity) at lower dopant concentration.

This trend of lower conductivity from pure zinc oxide to Fe doped zinc oxide may be due to carrier traps formation at the film surface causing impediment to charge carriers and due to Fe incorporation, with the formation of interstitial metal atoms causing a decrease in the oxygen vacancies (Cheng et al. 2016). Besides, increasing the concentration of Fe led to an increase in the number of surface defects in the zinc oxide matrix. This will result to the electrical resistivity of ZO being reduced as the concentration of Fe in ZO is increased slightly. Hence the conductivity is increased.

8.0 Conclusion

Doping with transition metals such as iron will significantly improve the structural, electrical, magnetic and optical properties of zinc oxide nano particles. As reported, the refractive index (n) decreased with increasing the Fe concentration of the doped zinc oxide nano-particles which correlated to the optical band gap behavior. Also, an increase of the saturation magnetization (Ms) values was noted with increase in Fe doped concentration. Furthermore, the resistivity of the zinc oxide nano-particles reduced as the concentration of Fe in ZO is increased slightly resulting in increase in the conductivity of the doped zinc oxide nano-particles.

References

Ashraf, R., Saira Riaz, Zohra Nazir Kayanib, Shahzad Naseem (2015) Structural and magnetic properties of iron doped ZnO nanoparticles. Materials Today: Proceedings 2 (2015) 5384 – 5389. doi: 10.1016/j.matpr.2015.11.055.

Carofiglio, M.; Barui, S.; Cauda, V.; Laurenti, M. Doped Zinc Oxide Nanoparticles: Synthesis, Characterization and Potential Use in Nanomedicine. Appl. Sci. 2020, 10, 5194; doi:10.3390/app10155194

Carofiglio, M.; Laurenti, M.; Vighetto, V.; Racca, L.; Barui, S.; Garino, N.; Gerbaldo, R.; Laviano, F.; Cauda, V. Iron-Doped ZnO Nanoparticles as Multifunctional Nanoplatforms for Theranostics. Nanomaterials 2021, 11, 2628. https://doi.org/10.3390/nano11102628

Chen, Z.C.; Zhuge, L.J.; Wu, X.M.; Meng, Y.D. Initial study on the structure and optical properties of Zn1-xFexO films. Thin Solid Films 2007, 515, 5462–5465. [CrossRef] https://doi.org/10.1016/j.tsf.2007.01.015

Cheng, W.; Ma, X. Structural, optical and magnetic properties of Fe-doped ZnO. J. Phys. Conf. Ser. 2009, 152, 012039. DOI 10.1088/1742-6596/152/1/012039

Cherifi, Y.; Chaouchi, A.; Lorgoilloux, Y.; Rguiti, M.; Kadri, A.; Courtois, C. Electrical, dielectric and photocatalytic properties of Fe-doped ZnO nanomaterials synthesized by sol gel method. Process. Appl. Ceram. 2016, 10, 125–135. DOI: 10.2298/PAC1603125C

Dhiman, P.; Chand, J.; Kumar, A.; Kotnala, R.K.; Batoo, K.M.; Singh, M. Synthesis and characterization of novel Fe@ZnO nanosystem. J. Alloys Compd. 2013, 578, 235–241. https://doi.org/10.1016/j.jallcom.2013.05.015

Ebrahimi, R., Hossienzadeh, K., Maleki, A., Ghanbari, R., Rezaee, R., Safari, M., … Puttaiah, S. H. (2019). Effects of doping zinc oxide nanoparticles with transition metals (Ag, Cu, Mn) on photocatalytic degradation of Direct Blue 15 dye under UV and visible light irradiation. Journal of Environmental Health Science and Engineering, 17(1), 479–492. doi:10.1007/s40201-019-00366-x

Faramawy, A.; Elsayed, H.; Scian, C.; Mattei, G. Structural, Optical, Magnetic and Electrical Properties of Sputtered ZnO and ZnO:Fe Thin Films: The Role of Deposition Power. Ceramics 2022, 5, 1128–1153. https://doi.org/10.3390/ceramics5040080

Fujimura, N.; Nishihara, T.; Goto, S.; Xu, J.; Ito, T. Control of preferred orientation for ZnOx films: Control of self-texture. J. Cryst.Growth 1993, 130, 269–279. https://doi.org/10.1016/0022-0248(93)90861-P

Hamid, S.B.A.; Teh, S.J.; Lai, C.W. Photocatalytic Water Oxidation on ZnO: A Review. Catalysts 2017, 7, 93. 1 – 14. doi:10.3390/catal7030093

Hwang, D.K.; Oh, M.S.; Lim, J.H.; Park, S.J. ZnO thin films and light-emitting diodes. J. Phys. D Appl. Phys. 2007, 40, R387–R412. DOI 10.1088/0022-3727/40/22/R01

Kumar, R.; Kumar, G.; Al-Dossary, O.; Umar, A. ZnO nanostructured thin films: Depositions, properties and applications—A review. Mater. Express 2015, 5, 3–23. doi:10.1166/mex.2015.1204

Kumar, S.; Kim, Y.J.; Koo, B.H.; Sharma, S.K.; Vargas, J.M.; Knobel, M.; Gautam, S.; Chae, K.H.; Kim, D.K.; Kim, Y.K.; et al. Structural and magnetic properties of chemically synthesized Fe doped ZnO. J. Appl. Phys. 2009, 105, 07C520. https://doi.org/10.1063/1.3073933

Liu, X.; Pan, L.; Zhao, Q.; Lv, T.; Zhu, G.; Chen, T.; Lu, T.; Sun, Z.; Sun, C. UV-assisted photocatalytic synthesis of ZnO–reduced graphene oxide composites with enhanced photocatalytic activity in reduction of Cr(VI). Chem. Eng. Journal. 2011, 183, 238–243. doi:10.1016/j.cej.2011.12.068

Madkhali, N. Analysis of Structural, Optical, and Magnetic Properties of (Fe,Co) Co-Doped ZnO Nanoparticles Synthesized under UV Light. Condens. Matter 2022, 7, 63. https://doi.org/10.3390/condmat7040063

Onu C.P, Ekpunobi A.J, Okafor C.E, Ozobialu L.A (2023) Optical Properties of Monazite Nanoparticles prepared Via Ball Milling. Asian Journal of Research and Reviews in Physics 7(4): 17 – 29. DOI: 10.9734/AJR2P/2023/v7i4146

Pan, H.; Yi, J.B.; Shen, L.; Wu, R.Q.; Yang, J.H.; Lin, J.Y.; Feng, Y.P.; Ding, J.; Van, L.H.; Yin, J.H. Room-Temperature Ferromagnetism in Carbon-Doped ZnO. Phys. Rev. Lett. 2007, 99, 127201. https://doi.org/10.1103/PhysRevLett.99.127201

Pashkevich AV, Fedotov AK, Kasyuk YV, Bliznyuk LA, Fedotova JA, Basov NA, Fedotov AS, Svito IA, Poddenezhny EN (2018) Structure and electrical properties of zinc oxide base iron doped ceramics. Modern Electronic Materials 4(3): 87–95. doi:10.3897/j.moem.4.3.39540

Elilarassi R. and Chandrasekaran, G. (2012) Synthesis and characterization of ball milled Fe-doped ZnO diluted magnetic semiconductor, Optoelectronics Letters, vol. 8, no. 2, pp. 109–112, 2012. Doi. 10.1007/s11801-012-1157-5

Ravichandran, K.; Karthika, K.; Sakthivel, B.; Jabena Begum, N.; Snega, S.; Swaminathan, K.; Senthamilselvi, V. Tuning the Combined Magnetic and Antibacterial Properties of ZnO Nanopowders through Mn Doping for Biomedical Applications. J. Magn. Magn. Mater. 2014, 358–359, 50–55. https://doi.org/10.1016/j.jmmm.2014.01.008

Rong, P.; Ren, S.; Yu, Q. Fabrications and Applications of ZnO Nanomaterials in Flexible Functional Devices-A Review. Crit. Rev. Anal. Chem. 2018, 49, 336–349. : https://doi.org/10.1080/10408347.2018.1531691

Salem, M.; Akir, S.; Ghrib, T.; Daoudi, K.; Gaidi, M. Fe-doping effect on the photoelectrochemical properties enhancement of ZnO films. J. Alloys Compd. 2016, 685, 107–113. https://doi.org/10.1016/j.jallcom.2016.05.254

Santos, D.A.A.; Macêdo, M.A. Study of the Magnetic and Structural Properties of Mn-, Fe-, and Co-Doped ZnO Powder. Phys. B Condens. Matter 2012, 407, 3229–3232. https://doi.org/10.1016/j.physb.2011.12.073

Shaban, M.; Zayed, M.; Hamdy, H. Nanostructured ZnO thin films for self-cleaning applications. RSC Adv. 2017, 7, 617–631. https://doi.org/10.1039/C6RA24788A

Shanmuganathan, G.; Banu, I.B.S. Influence of Codoping on the Optical Properties of ZnO Thin Films Synthesized on Glass Substrate by Chemical Bath Deposition Method. Adv. Condens. Matter Phys. 2014, 2014, 761960. https://doi.org/10.1155/2014/761960

Tereshchenko, A.; Bechelany, M.; Viter, R.; Khranovskyy, V.; Smyntyna, V.; Starodub, N.; Yakimova, R. Optical biosensors based on ZnO nanostructures: Advantages and perspectives. A review. Sens. Actuators B Chem. 2016, 229, 664–677. https://doi.org/10.1016/j.snb.2016.01.099

Theerthagiri, J.; Salla, S.; Senthil, R.A.; Nithyadharseni, P.; Madankumar, A.; Arunachalam, P.; Maiyalagan, T.; Kim, H.S. (2019) A review on ZnO nanostructured materials: Energy, environmental and biological applications. Nanotechnology 2019, 30, doi:10.1088/1361-6528/ab268a 392001.

Ueda, K.; Tabata, H.; Kawai, T. (2001) Magnetic and electric properties of transition-metal-doped ZnO films. Appl. Phys. Lett. 2001, 79, 988–990. https://doi.org/10.1063/1.1384478

Wang, C.; Chen, Z.; He, Y.; Li, L.; Zhang, D. (2009) Structure, morphology and properties of Fe-doped ZnO films prepared by facing-target magnetron sputtering system. Appl. Surf. Sci. 2009, 255, 6881–6887.https://doi.org/10.1016/j.apsusc.2009.03.008

Wang, D.; Chen, Z.Q.; Wang, D.D.; Gong, J.; Cao, C.Y.; Tang, Z.; Huang, L.R. (2010) Effect of thermal annealing on the structure and magnetism of Fe-doped ZnO nanocrystals synthesized by solid state reaction. J. Magn. Magn. Mater. 2010, 322, 3642–3647. https://doi.org/10.1016/j.jmmm.2010.07.014

Wu, X., Zhiqiang Wei, Lingling Zhang, Xuan Wang, Hua Yang, and Jinlong Jiang (2014) Optical and Magnetic Properties of Fe Doped ZnO Nanoparticles Obtained by Hydrothermal Synthesis. Journal of Nanomaterials. Volume 2014, Article ID 792102, 6 pages. http://dx.doi.org/10.1155/2014/792102

Xu, C., Cao, L., Su, G., Liu, W., Qu, X., & Yu, Y. (2010). Preparation, characterization and photocatalytic activity of Co-doped ZnO powders. Journal of Alloys and Compounds, 497(1-2), 373–376. doi:10.1016/j.jallcom.2010.03.076

Xu, Q.; Zhou, S.; Schmidt, H. (2009) Magnetic Properties of ZnO Nanopowders. J. Alloys Compd., 487, 665–667. https://doi.org/10.1016/j.jallcom.2009.08.033

Yusuf, Y.; Azis, R.S.; Mustaffa, M.S. (2019) Spin-Coating Technique for Fabricating Nickel Zinc Nanoferrite (Ni0.3Zn0.7Fe2O4) Thin Films. In Coatings and Thin-Film Technologies; IntechOpen: London, UK, 2019. DOI: 10.5772/intechopen.80461